Solution Properties of Biobased Hyperbranched Polyols Investigated by Multiple-Detection Size Exclusion Chromatography

Jelena Milic,[1] Iwao Teraoka,[2] Zoran S. Petrovic[1]

[1]*Kansas Polymer Research Center, Pittsburg State University, 1701 South Broadway, Pittsburg, Kansas 66762*
[2]*Polytechnic Institute, New York University, 333 Jay Street, Brooklyn, New York 11201*

Received 21 October 2011; accepted 11 January 2012
DOI 10.1002/app.36800
Published online in Wiley Online Library (wileyonlinelibrary.com).

ABSTRACT: We used multiple-detection size exclusion chromatography and batch-mode light scattering to follow the structural development of hydroxylated fatty acid methyl esters of soybean oil into hyperbranched (HB) polyol during polymerization by analyzing samples, collected at different times, in dilute solutions in tetrahydrofuran. The size of HB molecules was, as expected, smaller and more compact than that of their linear analogues of the same molecular weight (MW). Additionally, HB polyols were roughly spherical in shape. Plots of MW as a function of retention time and plots of the radius of gyration (R_g) as a function of MW showed an upturn; this indicated mixing of the high-MW components in late-eluting fractions, caused by either adsorption onto or trapping by the pore. For region of the plot before the turning points, the exponent in the Mark–Houwink equation was between 0.3 and 0.4. The exponent in the power relationship between R_g and MW was also below 0.5. It appeared that the shape of molecules for the same MW varied with the progress of the synthesis, as observed by a slope change in the viscometric radius dependence on MW for different HB polyol samples. © 2012 Wiley Periodicals, Inc. J. Appl. Polym. Sci. 000: 000–000, 2012

Key words: size exclusion chromatography (SEC); hyperbranched; light scattering; molecular weight distribution; solution properties

INTRODUCTION

Hyperbranched (HB) polyols synthesized from hydroxylated fatty acid methyl esters of soybean oil (hydroxylated biodiesel) and the development of their chemical properties (hydroxyl number, hydroxyl equivalent, and functionality) with time was described in our preceding article.[1] Briefly, hydroxyl groups were introduced into fatty acid methyl esters of soybean oil by the hydroformylation/hydrogenation process; this resulted in a mixture of monomers with one ester group and zero, one, two, and three hydroxyl groups. With the ester groups designated as A and the hydroxyls designated as B, we had a mixture of A ($\sim$ 15%), A–B (28%), A–BB (54%), and A–BBB (3%) types, which when heated, self-polymerized to polyols of different molecular weights (MWs), polydispersities, and functionalites. The structure of HB polymers depends on the composition of the starting mixture of fatty acids and their structures.[2] Because the composition of our starting mixture was well-defined and the process of synthesis was relatively simple with only a few side reactions, the resulting polyols had well-defined structures. In a mixture of A, A–B, A–BB, and A–BBB monomers, the latter two caused branching, A–B increased the MW while preserving functionality, and A decreased functionality while increasing MW. Although A–BB was a major component in our system, the presence of A–B and A monomers reduced the branching density. A specific feature of the HB polymers was the presence of dangling side chains that varied in length from 3 to 18 carbons; this was a result of different hydroxyl group positions in the fatty acids chains (A–B, A–BB, and A–BB) and the presence of nonfunctional fatty acids (A). These dangling chains may affect the viscosity (VI) of polyols and their crystallization behavior and solution properties. A ChemDraw-generated model of an HB polyol with a nominal MW of about 20,000 g/mol is shown in Figure 1.

The analysis of HB polymers explains how their structure evolves during the polymerization—how the shapes of the molecules, the packing density of the chains, and the transport properties (VI) vary with MW—and how they change with reaction time. In this article, we present an analysis of the molecular properties at different stages of polymerization in

Correspondence to: Z. S. Petrovic (zpetrovi@pittstate.edu).
Contract grant sponsor: United Soybean Board.

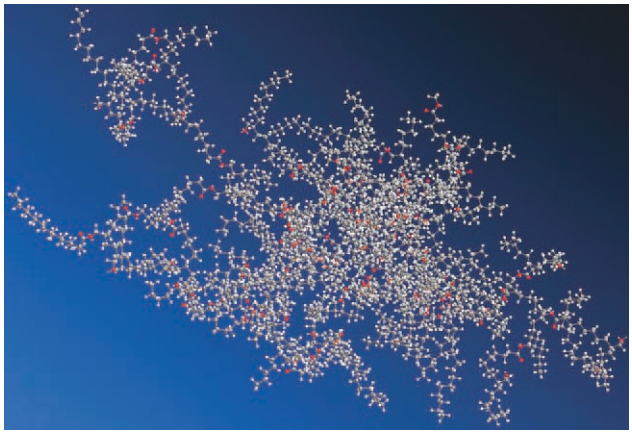

Figure 1 ChemDraw three-dimensional model of HB polyol with a MW of about 20,000 g/mol and the same fatty acid composition as the one in the feed. The energy was minimized with force field method MM2. [Color figure can be viewed in the online issue, which is available at wileyonlinelibrary.com.]

terms of different degrees of conversion of functional groups obtained from size exclusion chromatography (SEC) in combination with light scattering (LS), viscometry, and two concentration detectors: refractive index (RI) and UV.

The structure–property relationships in linear polymers are well known, but there are still challenges in understanding these relationships for more complex branched structures. The branching significantly changes the properties because of an increase in the average local density of repeat units compared with a linear polymer. Also, the segmental mobility of the branching points is lower compared with the other parts of the chain. Compared with a linear polymer having the same number of repeat units, the center of mass diffusion of the branched polymer is faster, and the VI is lower because of stronger hydrodynamic interactions, which facilitate the movement of nearby segments.

Currently, consistent classification of branched polymers is lacking because of their numerous possible topologies. HB polymers are considered a special case of dendritic polymers with a randomly developed branching architecture. Dendrimers, at the other extreme side, are characterized by a perfectly branched treelike structure, a well-defined functionality, and a controlled MW. Their unique properties and applications have attracted considerable interest over the past few decades.[3–14] However, their synthesis is difficult and expensive because it requires high monomer purity and a complex multistep synthesis.

In contrast, HB polymers have randomly branched topologies as a result of statistically driven polymerization in a one-pot synthesis. The preparation of HB polymers is easy and efficient; this makes these polymers suitable for large-scale, low-cost production. However, the simple synthesis method does not translate into a simple material.

Both dendrimers and HB polymers are composed of repeat units emanating from a central core. The functionality of the core is defined as the number of functional groups to which repeat units can be connected. For a dendrimer, the generation and the total number of repeat units defines the structure. For HB polymers, there are a large number of structures that can be formed from a given number of repeat units. This complexity leads to a broad distribution and diversity in MW, degree of branching, and chemical composition. Thus, establishing structure–property relationships is a challenging task from both the experimental and theoretical points of view.[15]

Significant development in the synthesis of HB polymers in the past few decades[2] has been followed by strong efforts to characterize and theoretically describe the properties of these materials and correlate them with their structures.[16–32] The most descriptive parameters of HB polymers are their MW and radius of gyration (R_g). Coupled with the information about internal structure, the combination of these data provides insight into the topological structure and allows for some prediction of their properties. Multiangle LS and online viscometry were used in this study to obtain values of the MW, R_g, second virial coefficient (A_2), and intrinsic viscosity ([η]).

EXPERIMENTAL

Materials

The HB polyester polyols[1] we obtained were designated as HB-3, HB-4, HB-5, and HB-6, where the number denotes the time in hours of the polymerization before the sample was taken for analysis. Details of the synthesis were described earlier.[1] Briefly, the synthesis used a multistep procedure, including the hydroformylation of soybean oil, the methylation of the hydroformylated oil, and then, the transesterification of hydroformylated methyl soyate. One of possible structures of the HB polyester polyol prepared from three major fatty acid methyl esters is shown in Figure 2.

A linear reference, necessary for estimating the degree of branching, was made by the self-condensation of hydroformylated methyl oleate. Poly(hydroformylated methyl oleate) (PHFMO) is actually a comb polymer with eight or nine carbons in each dangling side chain, shown in Figure 3. Dangling side chains, which also existed in the HB polyols but were not as uniform as in the linear reference, could affect the solubility and VI of the polymers.

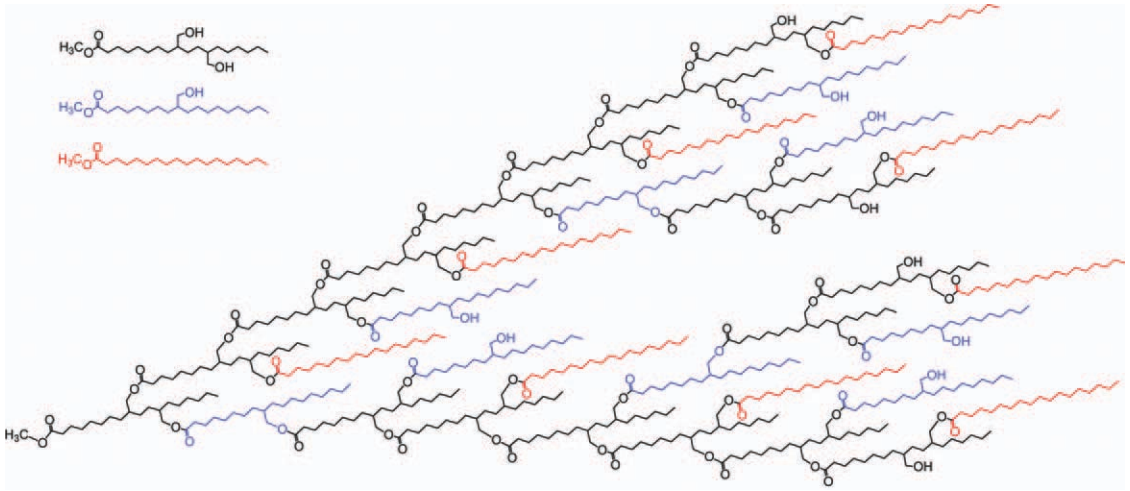

Figure 2 Structure of an HB polyester polyol with an MW of 10,976 g/mol and 10 OH groups. Three major components of fatty acid methyl esters are also displayed. [Color figure can be viewed in the online issue, which is available at wileyonlinelibrary.com.]

Methods

The solution properties of the HB polyols were analyzed with an SEC system. The system consisted of a pump (515, Waters Corp., Milford, MA), a manual 200-μL injector (Rheodyne, Rohnert Park, CA), a multiangle LS detector (Dawn EOS, Wyatt Technology Corp., Santa Barbara, CA), a differential refractometer (Optilab rEX, Wyatt), a VI detector (ViscoStar, Wyatt), and a UV–visible detector (SPD-20A, Shimadzu; 240 nm). Three Phenogel 5 μm columns (100, 1000 and 10,000 Å) plus a Phenogel guard column from Phenomenex (Torrance, CA, USA) covering a MW range of 10^2–10^6 were employed. The columns and detectors were thermostated at 30°C. Tetrahydrofuran (THF) was used as an eluent at a flow rate of 1.00 mL/min, as it had a sufficient RI contrast to the polymers and solubilized better than other polar solvents, such as acetonitrile and 2-butanone. We also tried chlorinated solvents, but these resulted in poor separation. The concentrations of the injected solutions varied from 29 to 13 mg/mL and were higher for lower MW samples. We confirmed that lower concentrations gave similar results, but with more scatter in the analysis results, such as MW and R_g. Analysis was performed in both online mode (with a multidetector SEC system) and batch mode (with the LS detector alone). ASTRA V 5.3.4.20 software (Wyatt) was used for data processing.

RESULTS AND DISCUSSION

Sensitivity of the detectors

Combined LS and RI detectors provided information about MW and R_g, whereas the VI detector in combination with the LS and RI detectors were used for assessing the transport properties of the molecules in solution. Figure 4 shows that the sensitivity of the the four detectors varies with MW or retention time. MW-sensitive detectors (VI and LS detectors) showed poor responses in the low-MW region of the

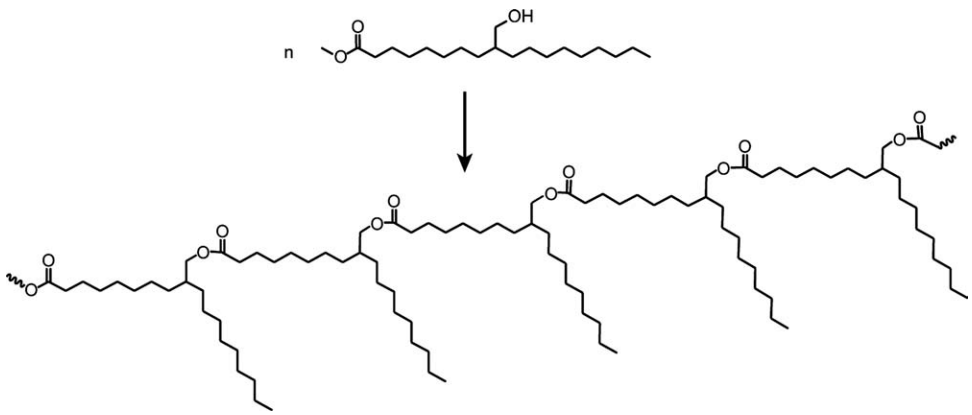

Figure 3 Synthesis of the linear reference: polyhydroformylated methyl oleate (PHFMO).

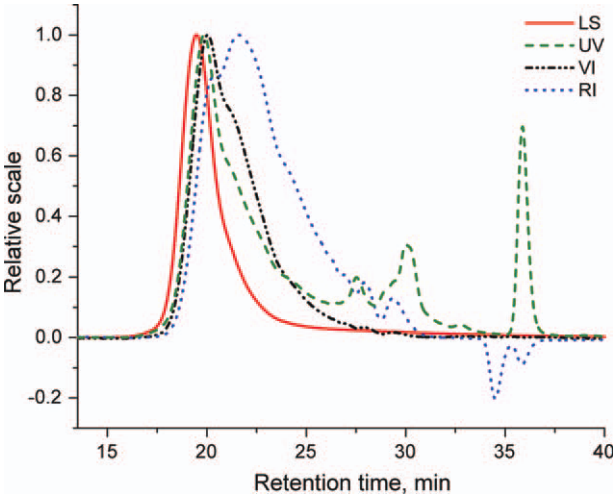

Figure 4 SEC curves of HB-5 by different detectors: LS (solid line), VI (dash-dotted line), RI (dotted line), and UV (dashed line). [Color figure can be viewed in the online issue, which is available at wileyonlinelibrary.com.]

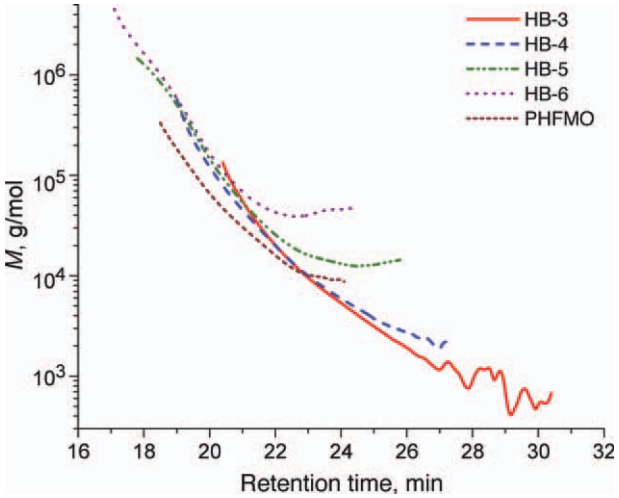

Figure 6 *M* plotted as a function of the retention time for the HB polyols and PHFMO. [Color figure can be viewed in the online issue, which is available at wileyonlinelibrary.com.]

chromatogram (retention time > 25 min), whereas the concentration-sensitive RI detector showed a weak response in the high-MW slice of the raw data (retention time < 19 min). These limitations compromised the estimation of the polymer properties at both ends of the chromatograms.

Molecular weight and MW distribution of HB polyols

Figure 5 compares the RI chromatograms of the four polyols. In the chromatograms of HB-3, HB-4, and HB-5, monomer, dimer, and trimer peaks were evident around 29.5, 28, and 27 min, respectively; this indicated that some unreacted monomers remained even at the late stages of the reaction. The low-MW peaks in the sample HB-6 were shifted and had somewhat different shapes with respect to those in the chromatograms of the other samples; this indicated different molecular structures of these late-eluting species. We speculated that they were a consequence of intramolecular rearrangements, possibly cyclization, in the late stages of the reaction involving transesterification. The chromatograms of HB-5 and HB-6 had two peaks between 19 and 22 min. This multimodal distribution was a consequence mainly of transesterification. However, another reaction, which occurred at the late stages, was interesterification, where ester–ester interchange led to the reconfiguration of molecules in the mixture to change the MW distribution without changing the number-average molecular weight (M_n).

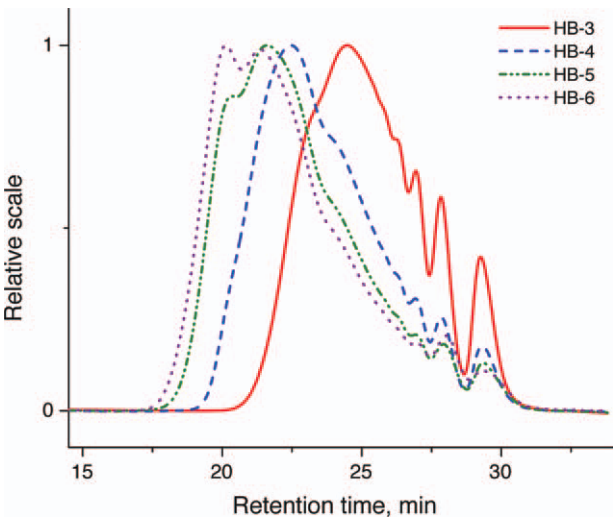

Figure 5 Chromatograms of HB-3 to HB-6 obtained with the RI detector. [Color figure can be viewed in the online issue, which is available at wileyonlinelibrary.com.]

Figure 6 shows a plot of the MW as a function of the retention time for the four polyols. Data are not displayed for the high- and low-MW ends of the chromatograms. First, we noticed that none of the curves followed a straight line. The same set of columns produced a nearly straight line when linear, broad-distribution polystyrene and poly(methyl methacrylate) (PMMA) were analyzed. Second, the four curves did not overlap with each other. If the polyol consisted of components having a similar architecture and the chain growth was similar throughout the polymerization, the four curves would lie along a master curve. The molecular structure of our polyol was diverse, and it changed with time during the reaction. This phenomenon indicated that molecules formed at different stages of the reaction had different structural morphologies when compared at the same MW. It appeared that at the early stages of reaction, the HB polyol

TABLE I
Average Molecular Weights and Refractive Indices of the HB Polyols and PHFMO[a]

Sample	M_n (g/mol)	M_w (g/mol)	M_w/M_n	dn/dc (mL/g)	n_D at 25°C
HB-3	2.1×10^3	5.5×10^3	2.6	0.079	1.472
HB-4	6.1×10^3	1.9×10^4	3.2	0.081	1.474
HB-5	2.3×10^4	6.9×10^4	2.9	0.081	1.475
HB-6	4.2×10^4	1.3×10^5	3.2	0.081	1.475
PHFMO	2.1×10^4	3.2×10^4	1.6	0.080	—

[a] Typical errors are ±1 of the last digit.

molecules had linear structures because of the length of fatty acids chains, whereas hyperbranching was prominent in molecules of a higher polymerization degree. Additionally, inter-esterification led to equilibration of the distribution because of the disintegration of molecules and their recombination; this gave different structures that varied with time.

The curves for HB-3 and HB-4 showed the expected behavior, that is, a decreasing MW with an increasing retention time in the whole range of MW (except at the very low-MW end). However, in HB-5 and HB-6, the curves had a turning point beyond which the MW increased with an increase in retention time.

A similar turning point in the plot of the MW as a function of retention time has been reported for branched polymers by several groups.[16,25,33–35] Some have ascribed it to the adsorption of some polymer components onto the pore surface,[16] whereas others have considered it as originating from the heterogeneity of the polymer structure[33–35] and leading to trapping by the tortuous pore structure. Both mechanisms may have occurred with our HB polyols, as we discuss later. The components eluted after the turning point were a mixture of long-retained components because of small molecular size and components that either adsorbed onto the pore of the column or were trapped by the tortuous pore structure. The presence of high-MW components in the late-eluting fractions increased the molecular weight (M), R_g, and other characteristic quantities. The effect on R_g was the most significant, as indicated in further discussion.

We wish to note that in Figure 4, the curve for the LS detector is tailing. The curve was nearly symmetrical when the broad distribution linear PMMA was separated. The tailing indicates that the late-eluting fractions contained a small amount of high-MW components. However, the M, R_g, and other quantities evaluated for each fraction were the mean values and were, therefore, significant even when the fractions were a mixture of different components.

Figure 6 also includes a curve for the PHFMO. The curve for PHFMO was below the curves for the polyols, except at the low-MW end. For the same M, the linear polymer eluted ahead of the branched polymer, a reasonable result.

The M_n, weight-average molecular weight (M_w), polydispersity index M_w/M_n, and specific refractive-index increment (dn/dc) for the four polyol samples and PHFMO were estimated in SEC and are summarized in Table I. Typical errors were ±1 of the last digit. The dn/dc, estimated with an assumption of 100% mass recovery, increased with MW and asymptotically approached a constant value at high MW. These values of dn/dc were identical to those obtained in the batch mode; this indicated that all of the polymer injected was released by the column.

For reference, we also measured the bulk refractive indices (n_D's) of the polymers at 25°C and 589.3 nm with an Abbe refractometer (Fisher Scientific, Pittsburgh, PA). The results are included in Table I. The RI detector of the SEC system used a 685-nm light source. The increase in dn/dc with increasing M_w and increase in n_D were consistent with each other.

Polydispersity index of the HB polyols

Unlike completely randomly branched polymers prepared in the condensation of multifunctional monomers, our HB polyols, with the average functionality of the starting components being about 1.3, had small polydispersity indices, with M_w/M_n = 2.6–3.2. The values were only slightly greater than 2 as a result of branching; this indicated that each polymer molecule consisted of primarily linear parts. Our monomers had two functional groups, hydroxyl and methyl ester, but only one methyl ester per molecule. Reaction could only occur between the methyl

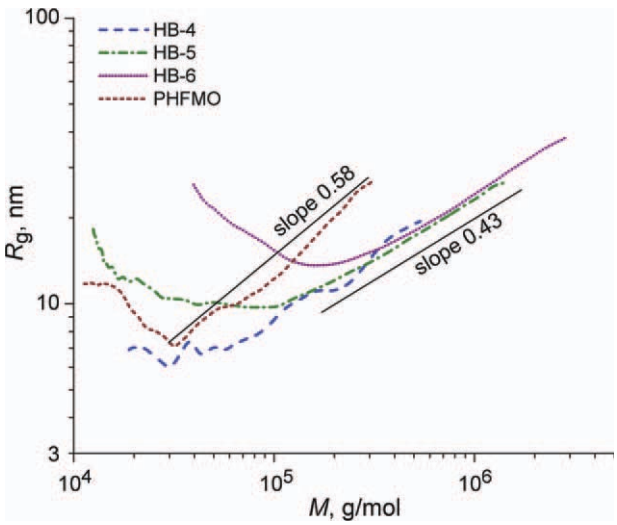

Figure 7 Dependence of R_g on MW for HB-4, HB-5, HB-6, and PHFMO. The slopes of the lines are 0.43 and 0.58. [Color figure can be viewed in the online issue, which is available at wileyonlinelibrary.com.]

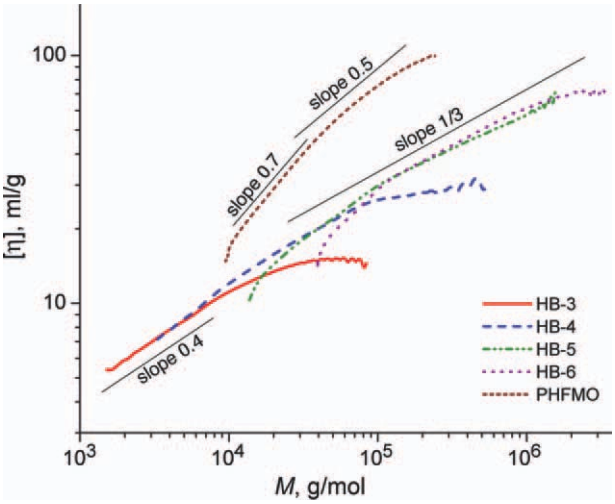

Figure 8 Mark–Houwink–Sakurada plot for the HB polyols and PHFMO. Straight lines are drawn to indicate the Mark–Houwink–Sakurada equations with specific slopes. [Color figure can be viewed in the online issue, which is available at wileyonlinelibrary.com.]

ester and hydroxyl, and there was no possibility of gelation. However, at long times and at high temperatures, ester–ester exchange (inter-esterification) could occur; this changed the MW distribution significantly.

Radius of gyration

Dependence of R_g on MW for HB-4, HB-5, HB-6, and PHFMO is presented in Figure 7. For most of the curve, HB-3 had an R_g below the detection limit of LS and is not included here. Except for the late-eluting components, the curves for the three polyols were on a straight line with a slope of 0.43; this indicated that the polymer conformation was somewhere between globular and linear, as expected for a highly branched polymer. The upturn observed in Figure 6 is more evident in Figure 7. The late-eluting components had a large average R_g. The upturn in the plot of R_g occurred at a smaller value of M compared with the upturn in Figure 6 because R_g was its z average, whereas M was its weight average. The difference between the two turning points indicated that the late-eluting fractions were a mixture of high- and low-MW components.

The curve for PHFMO also showed an upturn, but most of the curve before the upturn ran roughly along a line of slope of 0.58. However, the curve was not straight, and the behavior was far from the one typically observed for a linear polymer in a good solvent. Because R_g of PHFMO did not follow a straight line and its range of M was limited, we do not discuss the g parameter for our HB polyols further. Simply stated, R_g of the branched polyol was substantially smaller than that of PHFMO at the same M.

Rheological properties of the HB polyols

The Mark–Houwink–Sakurada equation relates [η] to M as follows:

$$[\eta] = K_\eta M^\alpha \tag{1}$$

where K_η and α are constants. Figure 8 shows [η] as a function of M in a double-logarithmic scale for four HB polyol samples and PHFMO. The parts after the turning points in Figure 6 are not displayed in Figure 8. The polyol samples followed a common envelope with a slope of the tangent around 0.4 for $M < 10^4$ g/mol and decreasing to around one-third for $M > 10^5$ g/mol. For each sample, the slope decreased to zero at the highest MW. The upward shift of the curves from HB-3 to HB-6 indicated that the majority of the branched polymer increased its dimensions and changed its shape during the reaction (as far as the dimension relevant to [η] is concerned). The small value of the slope, especially for the high-MW components, indicated that the polymer was compact and close to globular, at least for the majority of the molecule. A similar situation is illustrated in Figure 7. The downward deviation of [η] at the low MW in HB-5 and HB-6 was due to the presence of high-MW components in these late-eluting fractions.

The linear analogue, PHFMO, had a much greater [η] compared with the HB polyol of the same MW; this corroborated the compactness of the polyol molecules. Surprisingly, for $M < 4 \times 10^4$ g/mol,

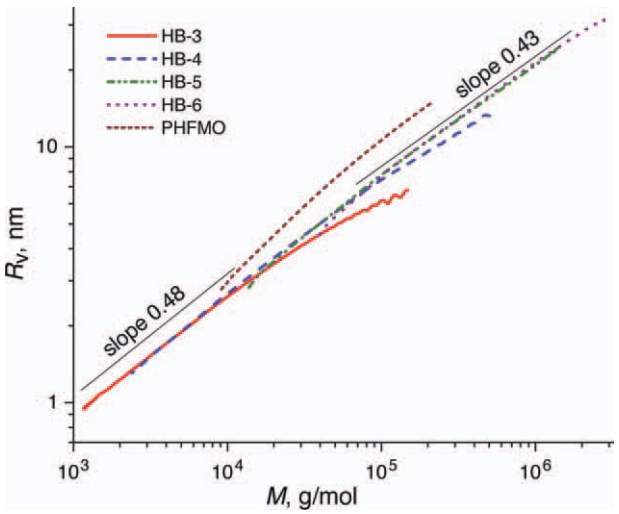

Figure 9 R_v versus MW for the HB polyols and their linear analogue. Slopes of 0.48 and 0.43 are indicated as straight lines. [Color figure can be viewed in the online issue, which is available at wileyonlinelibrary.com.]

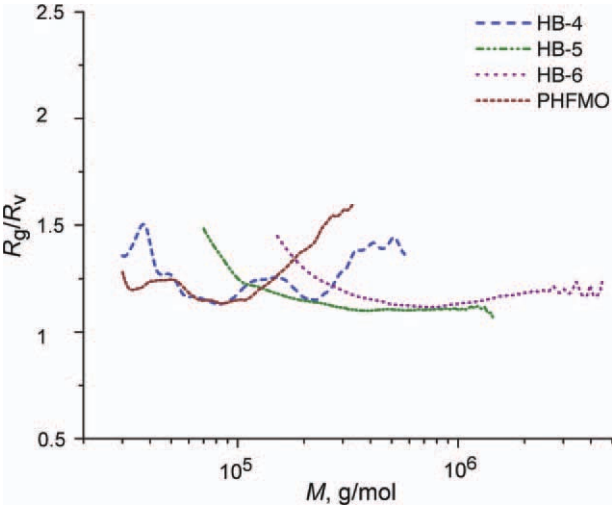

Figure 10 Ratio of R_g to R_v versus MW for HB-4, HB-5, HB-6, and PHFMO. [Color figure can be viewed in the online issue, which is available at wileyonlinelibrary.com.]

PHFMO followed a straight line of the slope close to 0.7, a typical value for linear polymers in a good solvent; our linear PMMA showed a straight line with a slope of 0.69. Above this MW, the slope gradually decreased to around one-third at $M = 2 \times 10^5$ g/mol. We considered that the solvent used (THF) was not effective in preventing PHFMO *n*-nonyl side chains from aligning with each other. The high-MW components of PHFMO were more globular than linear. The weak MW dependence of [η] of PHFMO (high-MW end) was mirrored or even more pronounced in the counterpart of the HB polyol samples. For each sample, [η] markedly deviated downward at the high end of the MW distribution. These high-MW components had [η] values that were fairly similar to the [η] values of the lower MW components. Recall that in contrast, R_g followed a straight line at the high end of the MW distribution. The high-MW components may have had linear-chain portions like antennas stemming from the dense core, and they were vulnerable to local side-chain alignment. Such a molecule will have a large R_g, but its [η] will remain small because the majority of the molecule exists in the core.

The viscometric radius (R_v) is determined from [η] by

$$R_v = \left(\frac{[\eta]M}{(10\pi/3)N_A}\right)^{1/3} \quad (2)$$

A suspension of solid spheres has an R_v value equal to its radius. In other words, R_v is the radius of a sphere in a suspension that has the same [η] as the polymer solution. Figure 9 shows a plot of R_v as a function of MW for both HB polyol samples and their linear analogue. Only the parts before the turning points in Figure 6 are displayed. The curves were similar to those in Figure 8, as expected. For the most part, the R_v values of the four polyol samples ran along an envelope curve that changed its slope of the tangent from 0.48 to 0.43 with increasing MW. For each polyol sample, there was a downward deviation at the high end of the MW distribution, but the deviation was less than it was in Figure 8. The linear chain had a greater R_v compared with polyol of the same *M*. Interestingly, the R_v values of PHFMO and HB-5 were straight toward the high end and followed a slope of 0.43.

The compactness of a molecule is commonly expressed by the size ratio to the linear analogue; however, information about the compactness can also be expressed by the introduction of a generalized ratio, R_g/R_v. The value is $(3/5)^{1/2} = 0.775$ for a suspension of solid spheres and 1.19 for a linear polymer in a θ solvent. The ratio was plotted as a function of *M* for the four polyol samples and PHFMO in Figure 10. Only the parts before the turning points in Figure 7 are displayed. The ratio rose strongly with decreasing *M*; this was ascribed to the mixing of high-MW components in later fractions. Otherwise, all of the samples, including PHFMO, had values close to the one for the linear polymer; this indicated that the overall shape of the branched polymer resembled that of a random coil. The decrease in R_g/R_v with increasing *M*, common to HB-4 to HB-6, was consistent with the difference between the slopes in Figures 7 and 9. In Figure 9, the slope for R_v changes from 0.48 to 0.43 with increasing *M*, whereas in Figure 7 the slope for R_g remains at around 0.43.

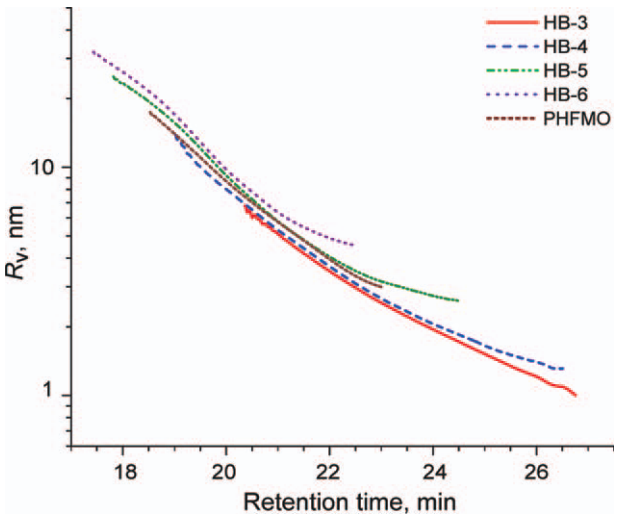

Figure 11 R_v plotted as a function of the retention time for the HB polyols and their linear analogue. [Color figure can be viewed in the online issue, which is available at wileyonlinelibrary.com.]

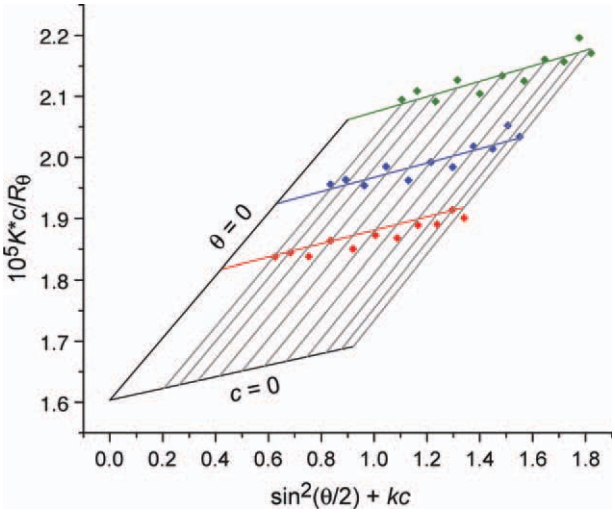

Figure 12 Zimm plot of HB-5 (scaling factor, k = 171.3 mL/g; c = 2.45, 3.68, and 5.25 mg/mL; and optical constant, $K^* = 3.72 \times 10^{-6}$ mol·cm^2/g^2). [Color figure can be viewed in the online issue, which is available at wileyonlinelibrary.com.]

Universal calibration

Figure 11 is a plot of R_v as a function of the retention time. Only the parts before the turning points in Figure 6 are displayed. If the separation in SEC is based on R_v, as is widely believed, all of the curves should lie along a master curve (universal calibration curve), but they did not. Even in the early elution, the fractions of the four polyol samples and PHFMO that eluted at the same time had different R_v's. The curve for HB-6 was higher than the curve for HB-5 and so on. The addition of repeat units to an existing polymer molecule increased R_v more than it increased the size recognized by SEC's pore. Such an addition is not possible with a linear polymer or dendrimer but is possible in an HB polymer as long as monomer remains in the reaction mixture and unreacted OH groups remain in the polymer molecule's core.

In the plot of R_g as a function of the retention time (not shown), overlap between the different curves was far worse; this indicated that R_v was still a better size parameter for SEC than R_g was.

A_2 values of the HB polyols

The experimental data shown thus far were obtained by SEC coupled with the LS, RI, and VI detectors. To estimate A_2, we carried out a batch LS mode for HB-5, HB-6, and PHFMO. The other two HB samples and PHFMO did not give reliable readings. To remove low-MW components, the PHFMO sample was fractionated, and only the fraction of the highest MW was used in the experiment. Several solutions of different concentrations in THF were prepared for each sample, and the Rayleigh ratio (R_θ) was measured as a function of concentration (c) and scattering angle (θ). The Zimm plot shown in Figure 12 for HB-5 allowed us to estimate M_w, R_g, and A_2. The results are summarized in Table II. The M_w of HB-6 was larger than the one listed in Table I. We noticed an early component in the chromatogram of the LS detector, but we did not include it in the estimates in Table I. That component could have contributed to the difference. The A_2 values of our polyols and their linear analogue were on the order of 10^{-4} mol·mL/g.

Another generalized size ratio, $A_2M_w/[\eta]$, was calculated for the samples. This ratio compares the volume of each polymer molecule estimated from the concentration dependence of the osmotic pressure to the one estimated from the concentration dependence of VI. Note that A_2M_w is a measure of the excluded volume of the polymer molecule and, hence, is sensitive to the longest linear dimension of the molecule in all directions. In contrast, [η] is contributed mostly by vicinal pairs of repeat units, as the hydrodynamic interaction between repeat units is reciprocally proportional to the distance between them. It is likely that a polymer with a large $A_2M_w/[\eta]$ has a dense core with extended antennas, consisting of mostly linear chains, and a polymer with a small $A_2M_w/[\eta]$ has a core only. For a sphere with hard-core repulsion, $A_2M_w/[\eta] = 8/5$. The large values of $A_2M_w/[\eta]$ in Table II, despite a small A_2, indicate that the polyols and the high-MW fraction of PHFMO had a dense core with extended antennas.

CONCLUSIONS

The solution properties of HB polyester polyols prepared from AB$_x$-type monomers removed from the reaction vessel at different stages of the reaction were investigated. Multiple-detection SEC was used to determine the average MW, MW distribution, size and shape of the molecules, and rheological properties of dilute solutions. For the HB polyester polyols, a relatively narrow MW distribution was found (2.6–3.2).

Batch-mode LS allowed us to estimate the polymer–solvent interaction. The A_2 values were positive but small.

TABLE II
M_w, R_g, A_2, and $A_2M_w/[\eta]$ of the HB Polyols and PHFMO (Highest MW Fraction)

Sample	M_w (g/mol)	R_g (nm)	A_2 (mol·mL/g^2)	$A_2M_w/[\eta]$
HB-5	$(6.2 \pm 0.1) \times 10^4$	17 ± 3	$(4.3 \pm 0.2) \times 10^{-4}$	1.6
HB-6	$(1.8 \pm 0.03) \times 10^5$	26 ± 2	$(8.0 \pm 2.0) \times 10^{-5}$	0.5
PHFMO	$(4.0 \pm 0.6) \times 10^5$	42 ± 4	$(1.7 \pm 0.3) \times 10^{-4}$	1.4

Chromatograms of late-stage polyol samples showed an upturn in MW and R_g, which was ascribed to either the adsorption of some high-MW components to the pore surface or trapping of the branched polymer by the tortuous pore structure. For the main part of the chromatograms that were not compromised by the upturn, HB polyol molecules were smaller than the linear analogues of the same MW.

The exponents in the power relationship in the plots of R_g versus M, [η] versus M, and R_v versus M were examined. The values of the exponents were a lot smaller than those for a typical linear polymer in a good solvent and were rather close to those of spheres. Thus, we found that the HB polyols were compact. We also compared R_g and R_v, and the results show that the HB polyols may have had linear chains extending from the core like antennas.

The polyol samples did not follow the universal calibration curve that nearly all linear polymers and long- and short-chain branched polymers follow. This result indicates that the separation in SEC was not based on the hydrodynamic volume. More studies with polyol samples prepared from different feeds are necessary to understand the retention mechanism.

References

1. Petrović, Z. S.; Cvetković, I.; Milić, J.; Hong, D.; Javni, I. J Appl Polym Sci, first published online : 31 JAN 2012, DOI: 10.1002/app.36232.
2. Gao, C.; Yan, D. Prog Polym Sci 2004, 29, 183.
3. Frechet, J. M. J.; Tomalia, D. A. Dendrimers and Other Dendritic Polymers; Wiley: Chichester, England, 2001.
4. Wu, C.; Ma, R.; Zhou, B.; Shen, J.; Chan, K. K.; Woo, K. F. Macromolecules 1996, 29, 228.
5. Cotts, P. M.; Guan, Z.; McCord, E.; McLain, S. Macromolecules 2000, 33, 6945.
6. Hudson, N.; MacDonald, W. A.; Neilson, A.; Richards, R. W.; Sherrington, D. C. Macromolecules 2000, 33, 9255.
7. Comanita, B.; Noren, B.; Roovers, J. Macromolecules 1999, 32, 1069.
8. Lepoittevin, B.; Matmour, R.; Francis, R.; Taton, D.; Gnanou, Y. Macromolecules 2005, 38, 3120.
9. Simon, P. F. W.; Muller, A. H. E.; Pakula, T. Macromolecules 2001, 34, 1677.
10. Patton, E. V.; Wesson, J. A.; Rubinstein, M.; Wilson, J. C.; Oppenheimer, L. E. Macromolecules 1989, 22, 1946.
11. Striegel, A. M.; Plattner, R. D.; Willett, J. L. Anal Chem 1999, 71, 978.
12. He, C.; Costeux, S.; Wood-Adams, P.; Dealy, J. M. Polymer 2003, 44, 7181.
13. Pavlov, G. M.; Korneeva, E. V.; Meijer, E. W. Colloid Polym Sci 2002, 280, 416.
14. Cao, X.; Sessa, D. J.; Wolf, W. J.; Willett, J. L. J Appl Polym Sci 2001, 80, 1737.
15. Burchard, W. Adv Polym Sci 1999, 143, 113.
16. Voit, B. I.; Lederer, A. Chem Rev 2009, 109, 5924.
17. Xinwu, B.; Ying, L.; Sujuan, W.; Haijun, W. Chin Sci Bull 2006, 51, 1526.
18. Cheng, K. C.; Chuang, T. H.; Tsai, T. H.; Guo, W.; Su, W. F. Eur Polym J 2008, 44, 2998.
19. Kratochvul, P. Pure Appl Chem 1982, 54, 379.
20. Vladimirov, N. In Encyclopedia of Chromatography, 3rd ed.; Cazes, J., Ed.; Taylor & Francis: New York, NY, 2009; p 559.
21. Ba, X.; Wang, H.; Zhao, M.; Li, M. Macromolecules 2002, 35, 3306.
22. Burchard, W. Macromolecules 1977, 10, 919.
23. Daoud, M.; J. F.Joanny. J. Physique 1981, 42, 1359.
24. Gaborieau, M.; Gilbert, R. G.; Gray-Weale, A.; Hernandez, J. M.; Castignolles, P. Macromol Theory Simul 2007, 16, 13.
25. Ioan, C. E.; Aberle, T.; Burchard, W. Macromolecules 2000, 33, 5730.
26. Ioan, C. E.; Aberle, T.; Burchard, W. Macromolecules 2001, 34, 3765.
27. Kulkarni, A. S.; Beaucage, G. Macromol Rapid Commun 2007, 28, 1312.
28. Nakao, T.; Tanaka, F.; Kohjiya, S. Macromolecules 2006, 39, 6643.
29. Nitta, K. H. Entropy 2009, 11, 907.
30. Tackx, P.; Bosscher, F. Anal Commun 1997, 34, 295.
31. Temyanko, E.; Russo, P. S.; Ricks, H. Macromolecules 2001, 34, 582.
32. Terao, K.; Farmer, B. S.; Nakamura, Y.; Iatrou, H.; Hong, K.; Mays, J. W. Macromolecules 2005, 38, 1447.
33. Podzimek, S.; Vlcek, T.; Johann, C. J Appl Polym Sci 2001, 81, 1588.
34. Wang, W.; Zheng, Y.; Roberts, E.; Duxbury, C. J.; Ding, L.; Irvine, D. J.; Howdle, S. M. Macromolecules 2007, 40, 7184.
35. Gerle, M.; Fischer, K.; Roos, S.; Muller, A. H. E.; Schmidt, M.; Sheiko, S. S.; Prokhorova, S.; Muller, M. Macromolecules 1999, 32, 2629.